

Design of Biocompatible Chitosan Microgels for Targeted pH-Mediated Intracellular Release of Cancer Therapeutics

Hong Zhang,[†] Sawitri Mardiyani,[‡] Warren C. W. Chan,^{*,†,‡,§} and Eugenia Kumacheva^{*,†,‡,§}

Department of Chemistry, University of Toronto, 80 Saint George Street, Toronto, Ontario M5S 3H6, Canada, Institute of Biomaterials and Biomedical Engineering, University of Toronto, 4 Taddle Creek Road, Toronto, Ontario M5S 3G9, Canada, Department of Materials Science & Engineering, University of Toronto, 184 College Street, Toronto, Ontario M5S 3E4, Canada, and Department of Chemical Engineering and Applied Chemistry, University of Toronto, 200 College Street, Toronto, Ontario M5S 3E5, Canada

Received November 29, 2005; Revised Manuscript Received February 12, 2006

We report the rational design of a chitosan-based drug delivery system. The chitosan derivative *N*-[(2-hydroxy-3-trimethylammonium)propyl]chitosan chloride (HTCC) was ionically cross-linked by sodium tripolyphosphate (TPP) to form sub-200-nm microgels that are responsive to pH changes. When these microgels were loaded with methotrexate disodium (MTX), a cytotoxic drug for cancer treatment, and conjugated to the targeting biomolecule apo-transferrin, a protein known to enter cells via receptor-mediated endocytosis, enhanced killing of immortalized HeLa cells was observed. In this intracellular delivery method, the microgel was exposed to low-pH environments that caused the chitosan to swell and release the drug. This rational drug delivery design may be useful in enhancing cancer therapy and reducing side effects.

Introduction

Design of polymer-based drug delivery systems (DDSs) for site-specific delivery and controlled release of therapeutics has attracted great interest from the chemical, materials science, and pharmaceutical communities.^{1,2} The programming of these two properties into the DDSs can dramatically improve drug efficiency and reduce side effects. Polymer-based DDSs can be classified into several groups such as polymer-drug conjugates,³ block copolymer vesicles and micelles,⁴ and sub-micrometer-size particles.⁵ Microgels, a subcategory of particulate DDSs, are particularly attractive for drug delivery: their size can be easily varied from 100 nm to several micrometers, their interior network can be used for the incorporation of drugs, and their surface can be conjugated to receptor-specific molecules to achieve targeting ability. Moreover, due to their open network structure, microgels carrying functional groups can undergo large swelling–deswelling transitions in response to changes in pH, ionic strength, or temperature. These changes are common in many biological events, and therefore, the engineering of a trigger-release system for drugs loaded into the microgels based on these events could dramatically improve therapeutic efficiency.

Synthetic pH-responsive microgel drug vehicles carrying acidic groups have been demonstrated.^{6,7} In an acidic environment these particles shrank, deformed, or precipitated to release the drug loaded in their interior. The current effort is aimed at the development of *biomicrogel* drug carriers: particles obtained from natural polymers that are biocompatible, nontoxic, and biodegradable⁸ (that is, after a particular time they undergo either

enzymatic degradation or nonenzymatic cleavage to be eliminated from the body). Furthermore, drug release “triggers” can be programmed into the biomicrogels by attaching specific functional groups to the polymer network. For example, pullulan acetate and sulfonamide-based microgels, containing the drug agent adriamycin, swelled in an acidic environment and killed MCF-7 human breast cells cultured in this acidic environment.⁹ It was suggested that these microgels could release a high drug dose in the tumor microenvironment, which can be acidic.

In this paper, for the first time we describe the rational design of pH-responsive chitosan-based microgels for intracellular targeted drug delivery. Chitosan (CS) and its derivatives, as precursors for preparing microgels, are attractive for synthesizing drug delivery systems. As a delivery vehicle, chitosan has mucoadhesive properties and this enhances drug penetration across intestinal epithelia.^{10,11} Beyond these properties, we can incorporate specific design features into the chitosan-based microgel to improve their delivery of tumor-killing drug agents. These design features would be based on recent studies and discoveries of basic tumor biology. These well-defined criteria are as follows: (a) the size of biomicrogels, which is important to the accumulation of the microgels in tumors *in vivo* (recent findings by Hobbs et al.¹² showed that ca. 200-nm-size particles have a higher accumulation efficiency at diseased sites than larger particles); (b) the targeted delivery of microgels by bioconjugating their surface with specific ligands that recognize receptors on diseased cells (recent research efforts have identified a large library for targeting agents to diseased sites)¹³; (c) the possibility of incorporating a drug in the interior of biomicrogels by physical means, that is, without chemical modification of the drug (the incorporation of drugs in delivery vehicles also protects them from enzymatic degradation); and (d) the ability of microgels to release the drug only under the action of a molecular or chemical stimulus (e.g., pH) (this ability should reduce side effects since cells will not be exposed to the drug molecules unless the drugs have been released from the carrier by a stimulus).

* To whom correspondence should be addressed. Phone: +1-416-978-3576 (and Fax; E.K.); +1-416-946-8416 (W.C.W.C.). Fax: +1-416-978-4317 (W.C.W.C.). E-mail: ekumache@chem.utoronto.ca (E.K.); warren.chan@utoronto.ca (W.C.W.C.).

[†] Department of Chemistry.

[‡] Institute of Biomaterials and Biomedical Engineering.

[§] Department of Materials Science & Engineering.

[§] Department of Chemical Engineering and Applied Chemistry.

While each of the characteristics of microgels demonstrated in the present work has been individually demonstrated for different DDSs, it is the combination of critical features (microgel size, sustained drug release, bioconjugation, and the use of biological degradable and biocompatible polymers) that made this material very promising for targeted drug delivery. In clinical use, the incorporation of these features into the biomicrogels DDSs should enhance the efficacy of the drug and reduce side effects.

Experimental Section

Materials. Chitosan (CS) with the molecular weight from 50 000 to 100 000 and degree of deacetylation of ~95% was donated by Yushan Ocean Biochemical Co. (Yuhuan, Zhejiang, China). Sodium tripolyphosphate (TPP), glycidyltrimethylammonium chloride (GTMAC), 1-ethyl-3-(3-dimethylaminopropyl)carbodiimide hydrochloride (EDC), bovine serum albumin (BSA), ninhydrin, methanol, ethanol, acetone, and Trypan Blue were purchased from Aldrich Canada. All of the chemicals used for preparation of water-soluble CdSe/ZnS quantum dots, such as DL-lysine, dicyclohexylcarbodiimide, and dimethyl sulfoxide (DMSO), were also obtained from Aldrich Canada. Methotrexate disodium (MTX) was purchased from Polymed Therapeutics, Inc. (Houston, TX). The deionized water was obtained from the Millipore Milli-Q water purification system.

Chitosan Modification. Chitosan powder (2.00 g) was dispersed in deionized water (5% (w/w)) at 85 °C. Glycidyltrimethylammonium chloride (7.35 mL) was added in three 2.45-mL portions at 2-h intervals.¹⁴ After 12 h, the solution was poured under stirring into cold acetone (200 mL) and then stored in the refrigerator for 6 h. Then, acetone was decanted, the remaining *N*-(2-hydroxy-3-trimethylammonium)propyl]chitosan chloride (HTCC) product was dried in air and dissolved in 60 mL of methanol. After addition of 250 mL of an acetone–ethanol mixture (4:1 (v/v)) HTCC was precipitated, filtered, and dried for 12 h in a vacuum oven.

Preparation of Microgels. A series of aqueous solutions of HTCC was prepared with concentrations of 0.10, 0.16, or 0.20 wt %. To a 5-mL HTCC solution, a TPP aqueous solution at various concentrations (0.05, 0.08, 0.12, and 0.16 wt %) was added dropwise under stirring with a speed of 700 ± 20 rpm. The weight ratios of HTCC/TPP were 4.0:1, 4.5:1, 5.0:1, and 5.5:1, respectively.¹⁰

Particle Characterization. The size and size distribution of microgels at various pH values were measured by using a DynaPro PCS spectrometer (Protein Solution Ltd., U.K.), equipped with a temperature controller. Electrokinetic potential of the microgels was determined by using photocorrelation spectroscopy (PCS; Zeta-sizer 3000HS, Malvern Instruments, U.K.). Morphology of HTCC microgels was characterized by using transmission electron microscopy on a Hitachi model 600 electron microscope at a 75-kV accelerating voltage. A droplet of microgel dispersion was placed onto a copper grid covered with carbon (Electron Microscope Sciences, Inc., USA) and allowed to dry.

Loading and Release of Drug. Methotrexate disodium was added to 2 mL of 0.16 wt % microgels under stirring at a speed of 500 ± 20 rpm. The weight ratios of MTX/HTCC were 0.30, 0.45, 0.60, and 0.80, respectively. The association efficiency (AE) and loading capacity (LC) were determined by isolating the microgels by ultracentrifugation and measuring the concentration of MTX remaining in the supernatant using UV–vis spectroscopy. The intensity of absorption for MTX was calculated at $\lambda = 372$ nm.

The release of MTX was determined over a 5-day time interval in a PBS buffer at pH = 7.4 and pH = 5.0. For each formulation 5 mL of MTX-loaded microgel dispersion was incubated for a certain time at 37 °C without stirring. At a specific time point, the microgel particles were separated from the buffer by ultracentrifugation at 24 000 *g* for 20 min. The concentration of MTX in the supernatant was measured by using UV–vis spectrometry. The amount of released MTX was determined by measuring the difference between the total amount of

loaded MTX and the amount of free MTX in the supernatant liquid. Each batch was analyzed three times.

Bioconjugation of Transferrin to Microgels. To each 100 μ L of 0.16 wt % HTCC microgel (180 nm in diameter) dispersion, 80 μ L of *apo*-transferrin solution with the concentration of 10 mg/mL was added in 0.01 M phosphate-buffered saline (PBS) at pH = 7.4. At least 10-fold molar excess of EDC was mixed for coupling. The reaction was maintained for at least 2 h. Then excess free EDC was removed by ultracentrifugation and replaced with the same amount of fresh PBS buffer.

Measurement of Transferrin Concentration. The amount of transferrin conjugated to the HTCC microgels was determined by a ninhydrin assay.¹⁵ Immediately after bioconjugation, the particles were centrifuged at 13 000 rpm for 15 min. A 100- μ L aliquot of the supernatant was mixed in a 96-well plate with 100 μ L of ninhydrin solution (50 mg/mL ninhydrin in ethanol). The plate was incubated at 50 °C for 20 min. The absorbance at 570 nm was read on a plate reader. We determined the transferrin concentration in the supernatant by comparing the absorbance signal to that of the calibration curve of ninhydrin assay of known concentrations of transferrin. These results allowed us to determine the concentration of transferrin on the surface of the microgel since the total concentration of transferrin in the reaction is known.

The number of particles per unit volume was estimated as V/v_i , where V is the total volume of particles per unit volume of dispersion (mL) and v_i is the mean volume of a particle. The value of V was found as

$$V = W/\rho \quad (1)$$

where W is the mass of “wet” microgel in a centrifuged dispersion and ρ is the density of wet microgel. Since the microgel particles were highly swollen in water, we assumed $\rho \approx 1.00$ g mL⁻¹. The value of v_i was determined as

$$v_i = (4/3)(\pi R_h^3) \quad (2)$$

where R_h is the hydrodynamic radius of HTCC microgel particles.

Incorporation of Quantum Dots. CdSe/ZnS QDs were synthesized and transferred to aqueous phase following the procedure described elsewhere.¹⁶ A few drops of CdSe/ZnS QDs in dilute aqueous solution were added into HTCC microgels after bioconjugation. The mixture was left for stirring for 6 h.

Drug-Loaded Microgel Assay. A 100- μ L aliquot of transferrin-conjugated MTX-HTCC microgels and control samples were pipetted into each cell dish (with ~1 million HeLa cells in a 60-mm tissue culture dish) and incubated at 37 °C for 24 h. The cells were trypsinized, washed with PBS twice, and stained with Trypan Blue. The numbers of live and dead cells were counted under an optical microscope (Olympus IX 71).

Results and Discussion

Figure 1 shows a schematic of the biomicrogels described in the present work. We synthesized 180-nm-diameter chitosan-based microgels (A), bioconjugated recognition molecules to the particle surface (B), and incorporated the anticancer drug agent MTX into the interior of the microgel (C). At reduced values of pH in the intercellular environment the microgels expanded and released MTX (D).

We used a two-step approach to prepare chitosan-based microgels that were stable at the biological pH value. In the first step, HTCC was obtained by grafting (2-hydroxyl) propyl-3-trimethylammonium to the CS backbone.¹⁷ In the second step, HTCC microgels were produced by conducting ionic association between the quaternary ammonia on the side chain of HTCC and TPP counterions.¹⁸ By changing the concentration of HTCC

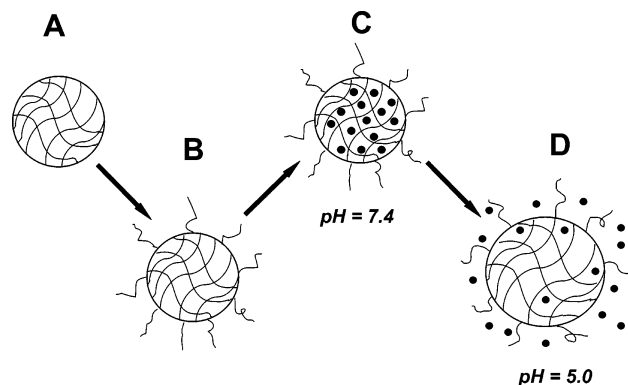


Figure 1. Schematic representation of the preparation of chitosan-based biomicrogels for targeted drug delivery and pH-responsive anticancer drug release: (A) preparation of CS-based microgels; (B) bioconjugation of CS-based microgels; (C) loading of bioconjugated CS-based microgels with a drug; (D) Swelling of bioconjugated CS-based microgels and release of the drug in endocytic vesicles with a pH = 5.0.

from 0.10 to 0.20 wt %, the concentration of TPP from 0.03 to 0.16 wt %, the weight ratio of HTCC/TPP from 6.5 to 4.5, and the degree of quaternization of HTCC from 75 to 95%, we tuned the mean hydrodynamic diameter of HTCC microgels from 180 to 800 nm.

Typically, a higher degree of quaternization of HTCC and higher degree of cross-linking led to a smaller size of microgels. The microgels were stable in 10 mM PBS at pH = 7.4. Figure 2a shows a typical transmission electron microscopy (TEM) image of the obtained microgel particles, which are single and spherical, and had a mean hydrodynamic diameter of ~180 nm in PBS buffers. We note that the microgel's polydispersity could be efficiently reduced by fractionating and deacetylating commercial chitosan.¹⁰

We investigated pH-responsive volume transitions of the resulting microgels at physiological temperature (37 °C). When the value of pH was reduced from 7.4 to 5.0, a 2.2-fold increase in hydrodynamic diameter and ca. 11.0-fold increase in volume was measured. (Figure 2b,c, respectively). Such change implied that the microgels will undergo strong swelling following their internalization into the cell and localizing in the lysosome or late endosomes if they entered the cells by receptor-mediated endocytosis. These organelles have pH values of $5 < \text{pH} < 6$.¹⁹ The increase in microgel size at low pH values originated from a higher degree of protonation of primary and secondary amino groups in HTCC thus increasing electrostatic repulsion within the polymer network. The increased protonation of amino groups was confirmed by measuring the electrokinetic potential (ζ -potential) of the microgels as a function of pH. The value of the ζ -potential increased from 12.5 to 35.7 mV in the range of pH from 7.4 to 2.5 (Figure 2b). Although the ζ -potential characterizes the surface charge of the particles, we assume that the amino groups in the interior of the microgel behave in a manner similar to the surface amino groups.

Since the values of $\text{pK}_{\text{a}3}$ and $\text{pK}_{\text{a}4}$ for TPP are 2.3 and 6.3, respectively,²⁰ in the range of $3 < \text{pH} < 6$, the change in microgel size originated mostly from the ionization of amino groups. When the value of pH approached 2.5, the concentration of TPP ions drastically reduced due to the protonation of TPP. This led to a lower degree of cross-linking in the microgel particles and thus a sharp increase in their size.

We incorporated the anticancer drug MTX in the interior of HTCC microgels (Scheme 1). At pH = 7.4 the negatively charged molecules of MTX were introduced into the positively

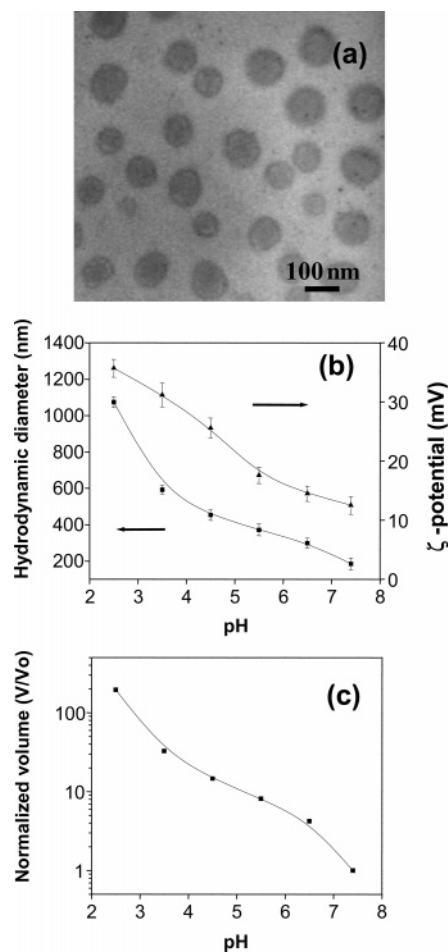
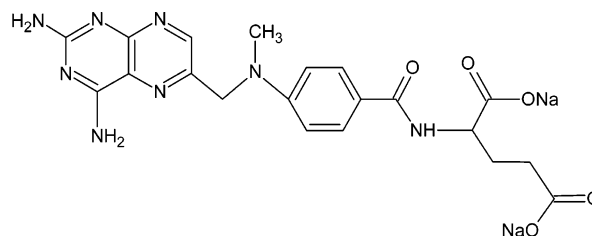


Figure 2. (a) Typical TEM image of HTCC microgels obtained by mixing 0.1 wt % aqueous solution of HTCC and 0.06 wt % aqueous solution of TPP at HTCC/TPP weight ratio of 5.0. (b) Variation in size (■) and ζ -potential (▲) of HTCC microgels in PBS buffers at various values of pH at $T = 37$ °C. (c) Variation in normalized volume of microgels as a function of pH. Normalized volume is defined as a volume of microgels at a particular value of pH divided by the volume at pH = 7.4. (Mean \pm SD, $n = 3$).

Scheme 1. Chemical Structure of Methotrexate Disodium



charged HTCC microgels via electrostatic forces. The CS microgel dispersions (polymer/TPP weight ratio of 5) were mixed with an aqueous solution of MTX at MTX/microgel weight ratio from 0.3 to 0.8 in PBS at pH = 7.4. We determined the LC of the microgels (defined as the weight of MTX loaded in the microgels divided by the microgel weight) and the AE of MTX (defined as the weight of the loaded MTX over the total weight of drug added to the system). The loading capacity increased with increasing MTX concentration in the PBS solution due to the increased concentration gradient (Figure 3a). The maximum LC of 52 wt % was reached at the MTX concentration of 1.26 mg/mL. The value of AE decreased with increasing MTX concentration, presumably, because the maximum absorption of the drug was reached. The maximum of AE was ca. 78 wt %.

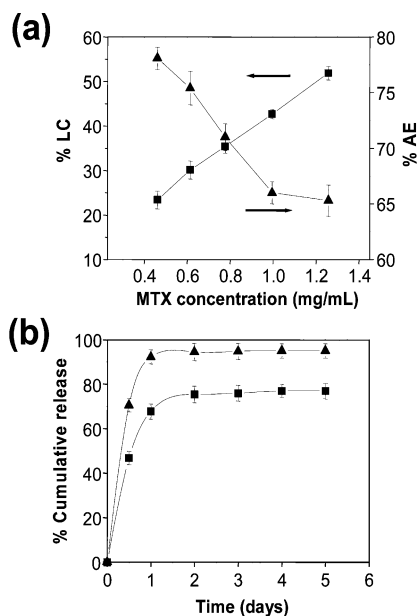


Figure 3. (a) Loading capacity (■) and association efficiency (▲) of CS-based microgels plotted as a function of MTX concentration. Microgel concentration is 0.16 wt %. (b) In vitro cumulative release of MTX from the microgels (LC = 41.2%) in PBS buffer at pH = 7.4 (■) and pH = 5.0 (▲). (Mean \pm SD, n = 3).

In vitro release of MTX from the interior of biomicrogels was investigated in PBS buffer solution at 37 °C. Figure 3b shows a cumulative release of MTX over a period of 5 days at pH = 7.4 and 5.0, respectively. Typically, for drugs loaded in polymeric drug carriers, the control of the drug release rate is based on diffusion of the drug and/or degradation of the drug carrier.²¹ In our work, the release of MTX was governed by the rate of diffusion of the drug from the polymer particles. At pH = 7.4 about 66% of MTX was released from the microgels within 1 day. After 5 days about 30% of the loaded drug was still trapped in the microgels via hydrogen bonding and ionic interactions between the MTX and the polymer. By contrast, in acidic conditions (pH = 5.0) a significantly faster release of MTX was achieved (ca. 93% after 1 day), with an almost complete release of ca. 95% within 3 days. Two factors favored faster and more complete release of the drug from the microgels at pH = 5. First, MTX was partly protonated at pH = 5 (the values of pK_{a1} and pK_{a2} of methotrexate disodium are 4.84 and 5.51, respectively²²); thus ionic interactions between MTX and the microgel became weaker. Second, at reduced pH, enhanced repulsion between the protonation of the amino groups of polymer molecules led to an increased pore size in the swollen microgel network, favoring diffusion of MTX.

We further conducted in vitro testing of the receptor-mediated intracellular uptake of the pH-responsive MTX-loaded HTCC microgel particles. In receptor-mediated endocytosis, a ligand binds onto a cellular receptor and becomes engulfed into the cell. The endocytic vesicles containing the ligands undergo a slow pH change, from 7.4 to 5.0, in the cells. We hypothesized that the pH change can induce the faster release of MTX stored in the microgel. As a proof-of-concept, we selected transferrin, a protein that enters cells through receptor-mediated endocytosis.²³ We used HeLa cells as a model cell line. The microgels were bioconjugated to *apo*-transferrin by EDC-mediated coupling in the PBS buffer at 7.4. The optimized reaction conditions for the EDC-mediated conjugation are at $4.7 < \text{pH} < 6$; however, the reaction with carbodiimide can also occur with at pH = 7.4 (although with a reduction in reaction efficiency).²⁴

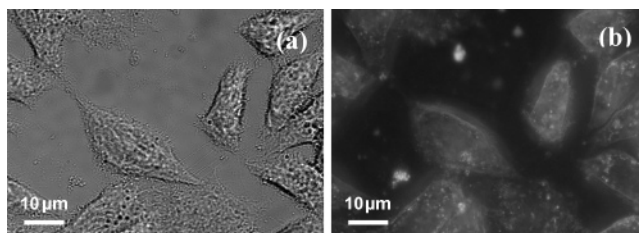


Figure 4. Differential interference contrast (a) and epifluorescent (b) images of HeLa cells after 4 h incubation with CdSe/ZnS QD-labeled transferrin-conjugated microgels. We used 100 \times objective, NA = 0.5 at λ_{ex} = 480 \pm 20 nm (100 W Hg lamp) and λ_{em} = 535 \pm 25 nm.

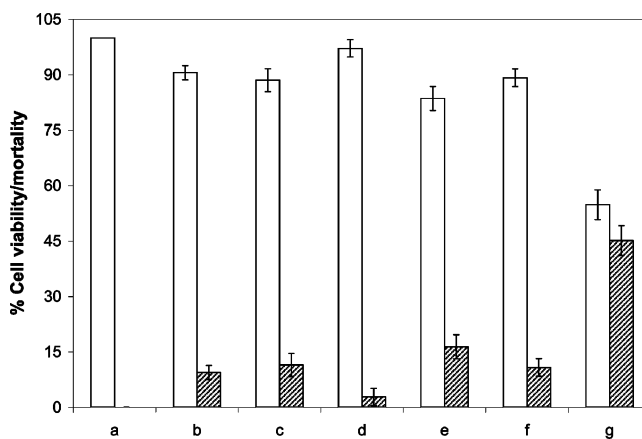


Figure 5. Viability (nonfilled)/mortality (striped) of (a) plain HeLa cells after 24-h incubation with (b) MTX, (c) HTCC microgels, (d) transferrin-conjugated HTCC microgels, (e) MTX-loaded HTCC microgels, (f) BSA-conjugated MTX-loaded HTCC microgels, and (g) transferrin-conjugated MTX-loaded HTCC microgels. (Mean \pm SD, n = 3).

Also, some of the transferrin may be nonspecifically adsorbed onto the surface of the microgel. We measured \sim 730 *apo*-transferrin molecules on the surface of each microgel particle. The activities of this protein on the microgel were not measured in these experiments, but previous studies show that *apo*-transferrin conjugated to nano- and microparticles is still able to recognize its receptor target and enter the cells after EDC-mediated conjugation.²⁵

To verify that the MTX-loaded microgels entered HeLa cells, we labeled the bioconjugated CS-based microgels with negatively charged luminescent semiconductor CdSe/ZnS quantum dots (QDs). Figure 4 demonstrates the targeting efficiency of *apo*-transferrin-conjugated microgels following their 4-h incubation. In Figure 4b the luminescence image featured discrete bright shapes, indicating that bioconjugated microgels were transported into the cells. In a control experiment carried out in the presence of QD-loaded *non*-bioconjugated microgels, a few or no bright spots were observed on/in the cells.

Finally, we investigated the efficiency of this bioconjugated microgel-based anticancer drug carrier for suppression of HeLa cells. Figure 5 depicts the results of a study of cell viability and mortality (that is, the percentage of survived and dead cells, respectively). HeLa cells were incubated for 24 h with (a) plain HeLa cells, (b) free MTX in amount calculated on the basis of the LC curve in Figure 3a (MTX concentration of ca. 1.02 mg/mL, LC \approx 45%), (c) HTCC microgels, (d) transferrin-conjugated HTCC microgels, (e) nonconjugated MTX-loaded HTCC microgels, (f) MTX-loaded HTCC microgels conjugated to BSA, and (g) transferrin-conjugated MTX-microgel complexes.

The mortality of the cells in these systems were 0, 9.4, 11.5, 2.8, 16.4, 10.8, and 45.2%, respectively. The transferrin-conjugated MTX-loaded CS-based microgels demonstrated a

significant (4.8- and 2.8-fold) increase in cell mortality of HeLa cells compared with the pure drug and non-bioconjugated MTX-loaded microgels. Two factors enhanced the efficiency of the biofunctionalized pH-responsive microgel drug carriers in suppressing HeLa cells. First, bioconjugated microgels were efficiently internalized into the cells through receptor-mediated endocytosis. Second, due to pH-induced swelling of the microgels, a faster diffusion-driven release of MTX was achieved in the acidic receptor-mediated endocytic vesicles.¹⁹

Conclusions

In the present work, we demonstrated the rational design of the drug delivery system based on a pH-responsive biomicrogels. The efficiency of suppression on HeLa cells was significantly enhanced by using the receptor-mediated endocytosis pathway and by triggering a faster release of the chemotherapeutic agent in the low-pH medium in the tumorigenic cells. In the future, this work will have implications in the design of vehicles for improving drug delivery and therapy to tumor sites as well as minimizing side effects.

Acknowledgment. E.K. thanks Canada Research Chair fund, NanoIP and CFI programs (NSERC Canada). W.C.W.C. acknowledges CIHR, NSERC, CFI, OIT, and the University of Toronto for financial support. H.Z. is grateful to the Ontario Graduate Scholarship Program (OGS). S.M. acknowledges the Canadian Federation of University Women and NSERC for graduate fellowships.

References and Notes

- (1) Uhrich, K. E.; Cannizzaro, S. M.; Langer, R. S.; Shakesheff, K. M. *Chem. Rev.* **1999**, 99, 3181–3198.
- (2) Kost, J.; Langer, R. *Adv. Drug Delivery Rev.* **2001**, 46, 125–148.
- (3) Batrakova, E. V.; Vinogradov, S. V.; Robinson, S. M.; Niehoff, M. L.; Banks, W. A.; Kabanov, A. V. *Bioconjugate Chem.* **2005**, 16, 793–802.
- (4) (a) Ahmed, F.; Dishcher, D. E. *J. Controlled Release* **2004**, 96, 37–53. (b) Moghimi, S. M.; Hunter, A. C.; Murray, J. C.; Szwedczyk, A.; Savic, R.; Luo, L. B.; Eisenberg, A.; Maysinger, D. *Science* **2004**, 303, 626–628. (c) Bronich, T. K.; Keifer, P. A.; Shlyakhtenko, L. S.; Kabanov, A. V. *J. Am. Chem. Soc.* **2005**, 127, 8236–8237.
- (5) Jung, T.; Kamm, W.; Breitenbach, A.; Kaiserling, E.; Xiao, J. X.; Kissel, T. *Eur. J. Pharm. Biopharm.* **2000**, 50, 147–160.
- (6) (a) Murthy, N.; Xu, M.; Schuck, S.; Kunisawa, J.; Shastri, N.; Frechet, J. M. J. *Proc. Natl. Acad. Sci.* **2003**, 100, 4995–5000. (b) Kohane, D. S.; Anderson, D. G.; Yu, C.; Langer, R. *Pharm. Res.* **2003**, 20, 1533–1538.
- (7) (a) Cai, T.; Hu, Z. B.; Ponder, B.; St. John, J.; Moro, D. *Macromolecules* **2003**, 36, 6559–6564. (b) Soppimath, K. S.; Tan, D. C. W.; Yang, Y. Y. *Adv. Mater.* **2005**, 17, 318–323. (c) Nayak, S.; Lee, H.; Chmielewski, J.; Lyon, L. A. *J. Am. Chem. Soc.* **2004**, 126, 10258–10259.
- (8) Pillai, O.; Panchagnula, R. *Curr. Opin. Chem. Biol.* **2001**, 5, 447–451.
- (9) Na, K.; Lee, K. H.; Bae, Y. H. *J. Controlled Release* **2004**, 97, 513–525.
- (10) Zhang, H.; Oh, M.; Allen, C.; Kumacheva, E. *Biomacromolecules* **2004**, 5, 2461–2468.
- (11) (a) Kumar, M. R. *React. Funct. Polym.* **2000**, 46, 1–27. (b) Agnihotri, S. A.; Mallikarjuna, N. N.; Aminabhavi, T. M. *J. Controlled Release* **2004**, 100, 5–28. (c) Calvo, P.; Remuñán-López, C.; Vila-Jato, J. L.; Alonso, M. J. *J. Appl. Polym. Sci.* **1997**, 63, 125–132. (d) Freiberg, S.; Zhu, X. X. *Int. J. Pharm.* **2004**, 282, 1–18.
- (12) Hobbs, S. K.; Monsky, W. L.; Yuan, F.; Roberts, W. G.; Griffith, L.; Torchilin, V. P.; Jain, R. K. *Proc. Natl. Acad. Sci. U.S.A.* **1998**, 95, 4607–4612.
- (13) (a) Lin, M. Z.; Teitell, M. A.; Schiller, G. J. *Clin. Cancer Res.* **2005**, 11, 129–138. (b) Houshmand, P.; Zlotnik, A. *Curr. Opin. Cell Biol.* **2003**, 15, 640–644. (c) Oishi, M.; Nagatsugi, F.; Sasaki, S.; Nagasaki, Y.; Kataoka, K. *ChemBioChem* **2005**, 6, 718–725.
- (14) Lim, S. H.; Hudson, S. M. *Carbohydr. Res.* **2004**, 339, 313–319.
- (15) Yemm, E. W.; Cocking, E. C. Ricketts, R. E. *Analyst* **1955**, 80, 209–214.
- (16) (a) Hines, M. A.; Guyot-Sionnest, P. *J. Phys. Chem.* **1996**, 100, 468–471. (b) Jiang, W.; Mardiyani, S.; Fischer, H.; Chan, W. C. W. *Chem. Mater.* **2006**, 18, 872–878.
- (17) Nam, C. W.; Kim, Y. H.; Ko, S. W. *J. Appl. Polym. Sci.* **1999**, 74, 2258–2265.
- (18) Xu, Y. M.; Du, Y. M.; Huang, R. H.; Gao, L. P. *Biomaterials* **2003**, 24, 5015–5022.
- (19) Killisch, I.; Steinlein, P.; Romisch, K.; Hollinshead, R.; Beug, H.; Griffiths, G. J. *Cell Sci.* **1992**, 103, 211–232.
- (20) Beukenkamp, J.; Rieman, W., III; Lindenbaum, S. *Anal. Chem.* **1954**, 26, 505–512.
- (21) Raman, C.; Berkland, C.; Kim, K.; Pack, D. W. *J. Controlled Release* **2005**, 103, 149–158.
- (22) Grim, J.; Chládek, J.; Martinková, J. *Clin. Pharmacokinet.* **2003**, 42, 139–151.
- (23) Chan, W. C. W.; Nie, S. M. *Science* **1998**, 281, 2016–2018.
- (24) (a) Hermanson, G. T. *Bioconjugate Techniques*; Academic Press: San Diego, CA, 1996. (b) Nakajima, N.; Ikade, Y. *Bioconjugate Chem.* **1995**, 6, 123–130.
- (25) (a) Yang, P.; Sun, X.; Chiu, J.; Sun, H.; He, Q. *Bioconjugate Chem.* **2005**, 16, 494–496. (b) Xu, Z.; Gu, W.; Huang, J.; Sui, H.; Zhou, Z.; Yang, Y.; Yan, Z.; Li, Y. *Int. J. Pharm.* **2005**, 288, 361–368.

BM050912Z